Bimetallic reactivity: unusual change in the coordination mode of the bridging ligands arising from an oxidative addition process

Miguel A. Ciriano, Jesús J. Pérez-Torrente, Fernando J. Lahoz and Luis A. Oro

Departamento de Química Inorgánica, Instituto de Ciencia de Materiales de Aragón, Universidad de Zaragoza (Consejo Superior de Investigaciónes Científicas), 50009-Zaragoza (Spain)

(Received December 10, 1993)

Abstract

The reactions of the dinuclear complex $[\{Rh(\mu\text{-}C_7H_4NS_2)(CO)(PPh_3)\}_2]$ (1) ($C_7H_4NS_2$ = benzothiazole-2-thiolate) with electrophilic agents have been studied. Iodomethane reacts with 1 to give the diacetyl complex $[\{Rh(\mu\text{-}C_7H_4NS_2)(COCH_3)(I)(PPh_3)\}_2]$ (2) as the result of the addition of one MeI molecule to each metal atom followed by the insertion of the carbonyl groups into the Rh–Me bonds. Monitoring this reaction by $^{31}P\{^1H\}$ NMR and IR shows that it goes through a dinuclear pathway. The crystal structure analysis of 2 shows a significant change in the coordination mode of the bridging benzothiazol-2-thiolates relative to the parent compound 1. In 2 each bridging ligand bonds through the exocyclic sulphur atom to both rhodium atoms, and the azolate nitrogen maintains a weak bonding interaction with one metal as shown by the long Rh–N distance, 2.588(3) Å. A further rearrangement is observed in solution, since spectroscopic studies show that 2 is in equilibrium with an acyl–mononuclear complex arising from the fragmentation of the dinuclear unit. Iodine also reacts with 1 to give the insoluble rhodium(III) complex $[\{Rh(C_7H_4NS_2)I_2(CO)(PPh_3)\}_n]$ whereas HgI_2 and methyl triflate react with 1 to give the heterotrinuclear and homotrinuclear aggregates $[(PPh_3)_2(CO)_2Rh_2(\mu_3\text{-}C_7H_4NS_2)_2HgI][HgI_3]$ (4) and $[Rh_3(\mu_3\text{-}C_7H_4NS_2)_2(CO)_3(PPh_3)_3]^+$ respectively, as a result of the attack of the electrophiles on the exocyclic sulphur atoms of the benzothiazole-2-thiolates.

Key words: Rhodium; Bridging ligands; X-ray structure; Oxidative addition; Benzothiazole-2-thiolato; diacetyl complex

1. Introduction

Dinuclear complexes are useful for testing the distinctive reactivity patterns of the multimetallic systems. When the metals are close the formation and breaking of a metal–metal bond, the insertion of small molecules into the metal–metal bond, the ligand mobility for terminal to bridging site and the transference of ligands from one centre to the other can be observed [1]. Looking for these effects, dinuclear ylide [2], bis-(diphenylphosphino)methane [3], thiolate [4], pyrazolyl [5], 3,5-bis(diphenylphosphinemethylene)pyrazolyl [6], 2-(diphenylphosphino)pyridine [7] and (diphenylphosphino)cyclopentadienyl [8] complexes have been studied.

Since oxidative addition and reductive elimination are fundamental steps in many catalytic cycles, much recent interest has been focused on dinuclear systems suitable for activating rather inert molecules [9]. Although the possible pathways of the oxidative addition reactions on these complexes depend on the nature of the metal (*i.e.* iridium(I) complexes usually give a "transannular" oxidative addition product [10]), the rigidity or flexibility of the framework of metals and bridging ligands also seems to be a crucial factor in metal–metal bond formation.

The design of new dinuclear complexes involves the use of new assembling ligands. In this context, we have studied bidentate bridging ligands having a N–C–S donor moiety, such as pyridine-2-thiolate and benzothiazole-2-thiolate [11], which have shown special ability to form dinuclear and trinuclear complexes. In addition, stabilization of unusual intermediates in oxidative addition reactions has also been observed [12]. To a large extent, the high flexibility of the eight-membered "$Rh_2(\mu\text{-}NCS)_2$" ring in these dinuclear complexes with *cis* bridging ligands allows a wide range of

Correspondence to: Prof. M.A. Ciriano.

0022-328X/94/$7.00
SSDI 0022-328X(94)24650-8

intermetallic distances. This flexibility and the presence of several basic sites have prompted us to study the reactivity of the complex $[\{Rh(\mu\text{-}C_7H_4NS_2)(CO)(PPh_3)\}_2]$ (**1**) towards some electrophilic reagents.

2. Results and discussion

The reactions of iodomethane, halogens, mercury(II) iodide and methyl trifluoromethanesulphonate with $[\{Rh(\mu\text{-}C_7H_4NS_2)(CO)(PPh_3)\}_2]$ (**1**) have been studied.

2.1. Reaction with iodomethane

Complex **1** does not react with dilute solutions of iodomethane in toluene, tetrahydrofuran or dichloromethane. The reaction is very slow and strongly dependent on the MeI concentration. Even at high MeI : Rh ratios (greater than 10 : 1), mixtures of several products are present in solution, and the starting material is always the predominant species. Nevertheless, when **1** is stirred in neat iodomethane, a brown solution is formed from which a red solid (**2**) begins to precipitate after 15 min. The optimum yield was found after 3 h. Longer reaction times result in lower yields owing to further reaction of **2** with MeI, leading to unidentified decomposition products.

The IR spectrum of **2** in the solid state shows no absorptions for terminal CO ligands but displays a broad band at 1695 cm^{-1} characteristic of acetyl groups. Microanalysis of **2** is consistent with the formulation $[\{Rh(C_7H_4NS_2)(COCH_3)(I)(PPh_3)\}_n]$ but the NMR spectra of **2** are puzzling. Its $^{31}P\{^1H\}$ NMR spectrum shows two doublets of unequal intensity centred at 40.3 and 35.1 ppm. The two different coupling constants (157 Hz and 140 Hz respectively) indicate that both phosphorus nuclei are coupled with the 100% active ^{103}Rh nucleus but not mutually coupled, which should indicate two different species in solution. In parallel, its ^1H NMR spectrum also shows two resonances of different intensities (1 : 2.3) for the acetyl groups, at 3.10 and 2.92 ppm respectively. After several recrystallizations of the reaction product from dichloromethane–hexane, the resulting red crystals showed spectra identical with those of the initial compound, suggesting that both species are in equilibrium in solution. The structure of **2** in the solid state classifies these observations.

Figure 1 shows a representation of the molecule $[\{Rh(\mu\text{-}C_7H_4NS_2)(COCH_3)(I)(PPh_3)\}_2]$ (**2**) together with the atom labelling. Selected bond distances and angles are collected in Table 1. The complex is dinuclear, with a crystallographically imposed twofold symmetry relating the two metal centres. The binary axis is perpendicular to the plane defined by the metals and

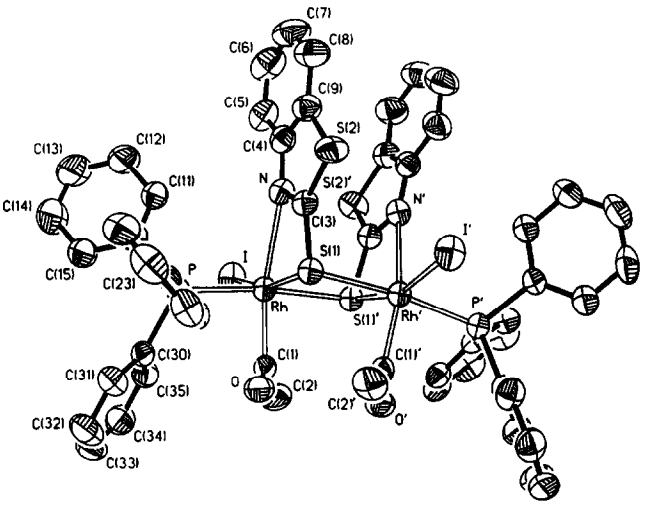

Fig. 1. Molecular representation of $[\{Rh(\mu\text{-}C_7H_4NS_2)(COCH_3)(I)(PPh_3)\}_2]$ (**2**) showing the numbering scheme.

the two exocyclic sulphur atoms. The rhodium atoms are directly bridged by two bonded sulphur thiolate atoms. Our description of the metal coordination sphere includes a rhodium–nitrogen interaction. On the assumption of a bonding interaction between the metal and the azolate nitrogen of the bridging ligand (see below), the metal coordination is distorted octahe-

TABLE 1. Selected bond distances (Å) and angles (°) for the complex $[\{Rh(\mu\text{-}C_7H_4NS_2)(COCH_3)(I)(PPh_3)\}_2]$ (**2**) (Primed atoms are related to the unprimed atoms by the symmetry transformation: $-x$, y, $0.5-z$)

Bond distances			
Rh–I	2.6617(3)	Rh–P	2.3288(9)
Rh–S(1)	2.3842(9)	Rh–C(1)	1.998(4)
Rh–S(1)′	2.4386(9)	Rh–N	2.588(3)
S(1)–C(3)	1.748(4)	C(1)–O	1.190(4)
S(2)–C(3)	1.731(4)	C(1)–C(2)	1.523(5)
S(2)–C(9)	1.749(4)	P–C(10)	1.826(4)
N–C(3)	1.296(5)	P–C(20)	1.828(3)
N–C(4)	1.381(5)	P–C(30)	1.836(4)
C(4)–C(9)	1.402(5)		
Bond angles			
I–Rh–S(1)	161.08(3)	S(1)–Rh–N	63.60(6)
I–Rh–S(1)′	90.86(2)	S(1)′–Rh–P	173.16(4)
I–Rh–P	91.53(2)	S(1)′–Rh–C(1)	85.1(1)
I–Rh–C(1)	101.4(1)	S(1)′–Rh–N	90.85(7)
I–Rh–N	99.46(6)	P–Rh–C(1)	88.1(1)
S(1)–Rh–S(1)′	81.52(3)	P–Rh–N	95.07(7)
S(1)–Rh–P	98.06(3)	C(1)–Rh–N	158.8(1)
S(1)–Rh–N	95.2(1)		
Rh–S(1)–Rh′	98.00(3)	Rh–C(1)–O	119.9(3)
Rh–S(1)–C(3)	87.7(1)	Rh–C(1)–C(2)	118.4(3)
Rh′–S(1)–C(3)	103.2(1)	O–C(1)–C(2)	121.6(3)
S(1)–C(3)–N	118.5(3)		

dral, with approximate relative *trans* positions as follows: the phosphine P atom to S(1)' (173.16(4)°). The iodine atom to S(1) (161.08(3)°), and the azolate nitrogen to C(1) (158.8(1)°). The whole molecular structure resembles that of the closely related $[Rh_2(\mu\text{-}C_7H_4NS_2)_2(CO)_3(PPh_3)]$ [13] with the additional presence of one iodine atom bonded to each metal atom and with the original bridging μ_2-1κN:2κS coordination modified to allow simultaneous coordination of the exocyclic S atom to both metals (μ_2-1κN, 1:2κS coordination mode).

The most intriguing feature of the structure is the long Rh–N separation: 2.588(3) Å. This value makes an immediate assignment of the electronic interaction between both atoms difficult, as this distance is significantly longer than those reported in related Rh complexes containing the same azolate ligand, *e.g.* 2.080(9) Å in $[(cod)_2Rh_2(\mu_3\text{-}C_7H_4NS_2)_2Ag(O_2ClO_2)]$ [11c], 2.040–2.045(4) Å in $(Ph_3P)Pt(\mu\text{-}C_7H_4NS_2)_2RhCl(CO)$ [14] or 2.136–2.150(17) Å in $[Rh_3(\mu_3\text{-}C_7H_4NS_2)_2(CO)_2(PPh_3)_2(tfbb)][ClO_4]$ [11b]. In spite of the long Rh–N distance, several factors imply some kind of bonding interaction between the nitrogen and the metal. First, this Rh–N distance is well inside (approximately 0.6 Å) the sum of the van der Waals radii of both atoms, 3.18 Å [15], and the N atom is in the region of an ideal sixth ligand of a distorted octahedron. Furthermore, the azolate nitrogen is *trans* to the acetyl group, which has been described as a high *trans* influence ligand [16]. This behaviour has been also clearly observed in the different Rh–N bond distances in acetylrhodium complexes as a function of the relative position of a nitrogen ligand: 2.034 and 2.112 Å in $[Rh(COCH_3)I\{GaMe_2(pz)(Me_2NCH_2CH_2O)\}]$ [17] and 2.121(11) Å in $[AsPh_4][Rh(COCH_3)I_3(CO)(py)]$ [18] in *cis* complexes, whereas this distance is significantly elongated to 2.31(1) Å for $[Rh(COCH_3)H\{N(CH_2CH_2PPh_2)_3\}]BPh_4$, the unique case where these ligands are *trans* [19]. In addition, the refined values of the displacement parameters for the nitrogen atom, which depend on the number of direct bonds established by each atom among other variables, are similar or even lower than those observed for the remaining triply bonded atoms of the molecule. None of these arguments by itself justifies the proposal, but all together make the existence of a weak bond between rhodium and nitrogen a sensible proposition.

The benzothiazole-2-thiolate exhibits a rather unusual bonding mode, μ_2-1κN, 1:2κS, acting as a five-electron donor and leading to the formation of three fused four-membered rings. Only three previous examples have been structurally characterized where this bridging ligand assumes this peculiar coordination. $[\{(M(CO)_3\}(\mu_2\text{-}C_7H_4NS_2)_2]$ (M = Mn or Re) [20], and $[\{Cd(\mu_2\text{-}C_7H_4NS_2)_2\}_n]$ [21]. In all these cases, the bridging ligands are roughly planar, with deviations

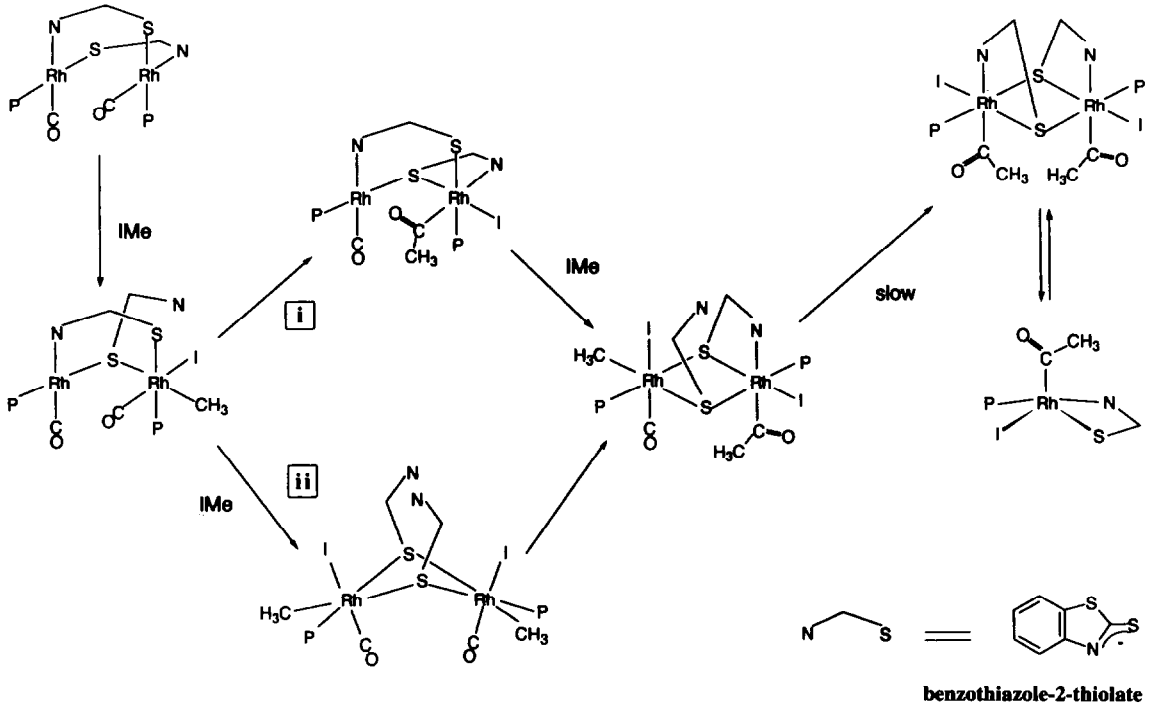

Scheme 1. Proposed mechanism for the reaction of $[\{Rh(\mu\text{-}C_7H_4NS_2)(CO)(PPh_3)\}_2]$ (1) with MeI.

from the least-squares plane through the benzothiazole moiety less than 0.41(6) Å (C(7) atom). The dihedral angle between the two symmetry-related benzothiazole-2-thiolate ligands is 15.97(3)°, considerably smaller than that observed in the closely related compound $[Rh_2(\mu\text{-}C_7H_4NS_2)_2(CO)_3(PPh_3)]$, 56.30(5)° [13]. The two Rh–S bond distances are different (2.3842(9) Å *vs.* 2.4386(9) Å) making the bridge slightly asymmetric, and the Rh_2S_2 ring is non-planar with a dihedral angle of 168.71(3)° between the Rh–S(1)–Rh′ and Rh–S(1′)–Rh′ planes. As usual for this donor or the closely related pyridine-2-thiol [22]—whatever the bonding mode—coordination causes a simultaneous lengthening of the exocyclic C–S, 1.748(4) Å, and a shortening of the C–N distance, 1.296(5) Å, compared with the free base, 1.662(4) Å and 1.353(6) Å, respectively [23]. Consistent with the proposed Rh–N bond, the C–N separation compares well with distances observed in transition metal complexes where the azolate nitrogen is clearly linked to the metals (mean, 1.32(2) Å) [24]. Both the exocyclic and endocyclic C–S bond distances are very similar, indicating that this type of coordination delocalizes the π electrons with a substantial loss of multiple-bond character in the exocyclic C–S bond.

As expected, the Rh–P bond distance, 2.3288(9) Å, is slightly longer than the separation observed in the Rh(I) complex $[Rh_2(\mu\text{-}C_7H_4NS_2)_2(CO)_3(PPh_3)]$ [13], and compares well with the values determined for hexacoordinated Rh(III) compounds (mean, 2.32(4) Å). The Rh–I distance and the structural parameters involving the acetyl ligand are normal and deserve no further comment [16b,25].

The complex $[\{Rh(\mu\text{-}C_7H_4NS_2)(COCH_3)(I)(PPh_3)\}_2]$ (**2**) is the consequence of an oxidative addition of MeI onto each metal atom followed by a double methyl migration to give the diacetyl complex. As mentioned above, solutions of **2** contain two species, but a reversible decarbonylation of the acetyl groups is excluded because its IR spectrum shows no absorptions for terminal carbonyl groups and a broad band at 1720 cm^{-1} is displayed instead. The shift to higher frequencies of ν(CO) in solution relative to the solid state (25 cm^{-1}) may indicate different environments around the metals.

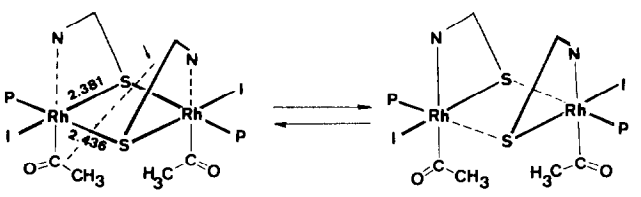

Fig. 2. Asymmetric dimetallic core of **2** suggesting the bond-breaking scheme leading to mononuclear fragments in solution.

A reasonable explanation for this behaviour is an equilibrium between dinuclear and mononuclear species (Scheme 1). The dinuclear species has two benzothiazole-2-thiolate bridging ligands but in the mononuclear complex this ligand is bidentate and chelating. In both cases, pentacoordination around rhodium would result from the large *trans* influence of the acetyl group [16], in accordance with the shift of ν(CO) mentioned above. Most mononuclear rhodium acetyl complexes are pentacoordinate although X-ray structures for this type of compound are scarce. Both trigonal–bipyramidal and square–pyramidal arrangements are known. For example, $[Rh(COCH_2CH_2Ph)Cl_2(PPh_3)_2]$ [26] and $[RhI(\eta^2\text{-}S_2PPh_2)(COMe)(PPh_3)]$ [27] have a square–pyramidal structure with an apical acyl group, whereas $[Rh(COCH_2Ph)Cl_2(PPh_3)_2]$ [28] and $[(PP_3)Rh(COCH_3)]$ (PP_3 = tris(diphenylphosphinoethyl)phosphine) [29] display trigonal–bipyramidal structures. Nevertheless, square–pyramidal is preferred when a chelating ligand is involved, as proposed for dithiolate complexes $[Rh(S\text{–}S)(COCH_3)\{P(4\text{-}XC_6H_4)_3\}_2]$ (S–S = S_2COMe^- or $S_2CNEt_2^-$; X = F, Cl, Br or I) [30].

The suggested dissociation of **2** (Scheme 1) is supported by the following observations: Both species are identified in the mass spectrum fast atom bombardment (FAB) of a solution of **2**, and the mononuclear complex shows sequential loss of iodo and acetyl fragments. The equivalence of both acetyl groups and benzothiazol-2-thiolate ligands in the ^1H NMR spectrum of **2** for the main species suggests C_{2v} symmetry. This, together with the one single distinctive down-field resonance of the H(4) protons (sensitive to the coordination mode of the benzothiazol-2-thiolate) [14], indicates bridging (N,S) coordination in the main species and chelation of this ligand in the minor species.

The asymmetric S–Rh core and the Rh–N bonding interaction found in the solid state structure suggest both the breaking of the two longest Rh–S bonds in solution and the subsequent strengthening of the Rh–N bonds to give the mononuclear complex (Fig. 2). Alternatively, strengthening of the Rh–N bonds would lead to breaking of the short Rh–S bonds to give a less strained dinuclear complex with pentacoordinated metals.

The evolution of the reaction of **1** in neat MeI, was monitored by $^{31}P\{^1H\}$ NMR spectroscopy. As shown in Fig. 3, the intensity of the resonance (A) corresponding to the starting material decreases as the final products (resonances E and F) are formed. Unfortunately **2** crystallized out during the experiment and prevented any kinetic study, but some qualitative features of this

reaction can be inferred. The dinuclear complex (resonance E) is observed before the mononuclear complex (resonance F) appears, which indicates (i) that the equilibrium between the mononuclear and dinuclear species is reached from the dinuclear complex and (ii) that dinuclear species should be involved in the intermediate steps. In addition, two intermediates in the reaction are detected: the weak resonances B ($\delta = 44.2$ ppm) having a large coupling constant ($^1J_{Rh-P} \approx 180$ Hz) are attributed to the first intermediate since they appear at the beginning of the reaction and disappear just when all the starting material has been consumed. The resonances C ($\delta = 43.1$ ppm; $^1J_{Rh-P} = 171$ Hz) and D ($\delta = 27.4$ ppm; $^1J_{Rh-P} = 123$ Hz), of equal intensities, are assigned to the second intermediate, which is probably the dinuclear compound $[(PPh_3)(CO)(CH_3)(I)Rh^{III}(\mu\text{-}C_7H_4NS_2)_2Rh^{III}(COCH_3)(I)(PPh_3)]$. This formulation is supported by the observation of absorptions at 2055 and 1720 cm^{-1} in the IR spectrum of the reaction mixture corresponding to terminal carbonyl and acyl which appears at the same time as resonances C and D. No other IR bands from the reaction mixture are observed in the 2200–1600 cm^{-1} region except that of the starting material at 1985 cm^{-1} and those of the MeI at 2155 and 1755 cm^{-1}.

These observations are rationalized by the proposed mechanism for the reaction (Scheme 1). We suppose that the reaction starts with the oxidative addition at one metal. Spontaneous insertion of carbon monoxide into the Rh–Me bond occurs if there is a *cis* arrangement of CO and alkyl group after the oxidative addition. This methyl migration should be very fast, as described for mononuclear rhodium complexes containing chelating N,S ligands [31]. In this well-studied reaction [32], a *trans* ligand to the alkyl group of sufficiently high *trans* influence to weaken the metal–alkyl bond is usually necessary. This role is attributed by Leipoldt and coworkers [31] to sulphur donor atom. Sometimes an incoming or external nucleophile may promote the reaction since it fills the vacant site in the unsaturated acyl complex produced after the alkyl migration to the carbonyl group [33]. The response to the coordination vacancy in a dinuclear system should be even more complex, since a donor–acceptor metal–metal bond *trans* to the acyl group can be formed [34], as observed by Poilblanc and coworkers [8d] in the complex $[(CH_3CO)Rh^{II}(\mu\text{-}CpPPh_2)_2Rh^{II}(CO)]^+$.

In our case, the response to unsaturation could be participation of the benzothiazol-2-thiolate ligand. We believe that a change in the coordination mode of one bridging ligand from an N,S donor to form an S-thiolate bridge occurs simultaneously with the first oxidative addition. We and others have shown previously that this kind of change in coordination occurs in dinuclear pyridine-2-thiolate-bridged rhodium and palladium complexes [35]. The uncoordinated nitrogen

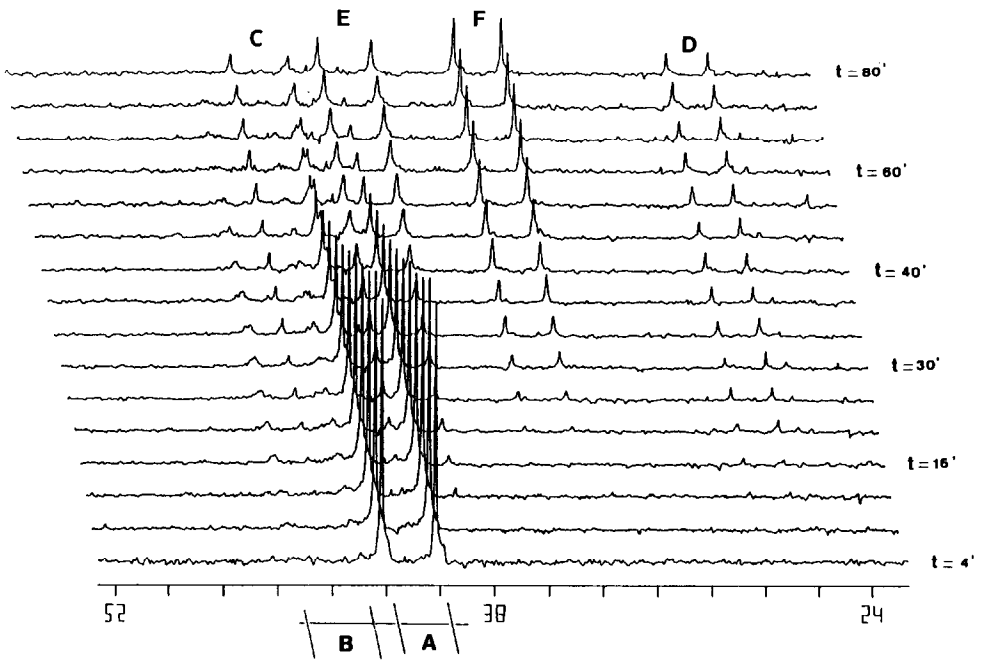

Fig. 3. Evolution of the reaction mixture between $[\{Rh(\mu\text{-}C_7H_4NS_2)(CO)(PPh_3)\}_2]$ (1) and iodomethane monitored by $^{31}P\{^1H\}$ NMR.

atom should then play the role of "incoming ligand" which also contributes to the carbonyl insertion. An alternative but less probable reaction pathway leading to the proposed intermediate could be (ii). In this context, oxidative addition of MeI to the related thiolate-bridged dinuclear rhodium complexes $[\{Rh(\mu\text{-}S^tBu)(CO)(PMe_2Ph)\}_2]$ does not take place at the second metal, and the final product of this reaction is the monoacetyl complex $[Rh_2(\mu\text{-}S^tBu)_2(COMe)I(CO)(PMe_2Ph)_2]$ [4a]. MeBr gives the monoacyl methyl complex $[Rh_2(\mu\text{-}S^tBu)_2(COMe)MeBr_2(CO)(PMe_2Ph)_2]$ under forcing conditions. In any case, the rate-limiting step of the reaction is the second carbonyl insertion in the metal–methyl bond. This makes that the second intermediate accumulate as the reaction proceeds. Finally, the dinuclear complex breaks into two mononuclear complexes to give the above-mentioned equilibrium, in which only one of the possible isomers is detected.

2.2. Reaction with halogens

Iodine (in a molar ratio I_2 : Rh = 1 : 1) reacts instantaneously with **1** leading to a red–brown precipitate which is analysed as $[\{Rh(C_7H_4NS_2)I_2(CO)(PPh_3)\}_n]$ (**3**). The low solubility of the product in common organic solvents precluded further characterization. Nevertheless, solutions of the reaction mixture (before isolation) allowed us to analyse of the spectroscopic properties of the complex. The $^{31}P\{^1H\}$ NMR spectrum shows a doublet centred at 39.0 ppm ($^1J_{Rh-P}$ = 93 Hz) consistent with a single or equivalent phosphorus nuclei. The IR spectrum in dichloromethane solution shows a sharp absorption at 2080 cm^{-1}. The large shift of the CO stretching frequency compared with the starting material (1985 cm^{-1}) and the reduction in the coupling constant compared with **1** ($^1J_{Rh-P}$ = 162 Hz) clearly indicate an increase in the formal oxidation state of both rhodium atoms. Moreover, the large difference observed (69 Hz) suggests changes in the electron density around the rhodium atom. Fragmentation of the starting dinuclear unit to give a mononuclear complex $[Rh(C_7H_4NS_2)I_2(CO)(PPh_3)]$, having the benzothiazole-2-thiolate ligand chelating probably occurs. When a lower molar ratio I_2 : Rh (1 : 2) is used, mixtures containing **3** and unreacted starting material are formed, as deduced from ^{31}P NMR and IR monitored experiments. In addition, **3** is the only species detected in solution when a large excess of iodine is added.

Complex **1** also reacts with Cl_2 and Br_2 (molar ratio X_2 : Rh = 1 : 1) to give intractable mixtures of products. No simple mixtures are obtained on increasing the Br_2 : Rh ratio but bubbling Cl_2 gas through a dichloromethane solution for 3 min allowed us to isolate the complex $[\{Ru(\mu\text{-}Cl)Cl_2(CO)(PPh_3)\}_2]$ [36] with a good yield (over 60%). In this case, the double oxidative addition is followed by a formal replacement of the benzothiazole-2-thiolate bridging ligands by chloride. These results correlate well with the oxidation power of the corresponding halogen.

2.3. Reaction with mercury(II) iodide

Interaction of mercury(II) halides with d^8 metal complexes usually leads to metal–mercury bonds as result of oxidative addition [37]. However, sometimes Lewis acid–base adducts are formed [38]. Complex **1** reacts with 2 equivalents of HgI_2 to give the cationic trinuclear aggregate $[(PPh_3)_2(CO)_2Rh_2(\mu_3\text{-}C_7H_4NS_2)_2(HgI)][HgI_3]$ (**4**). Characterization is based on its mass spectrum which shows the molecular ion at 1446 (9%, M^+). The presence of a peak at 583 (100%) in the negative FAB mass spectrum showing the expected fine structure supports the formulation of $[HgI_3]^-$ as counteranion The IR spectrum in dichloromethane shows a sharp absorption at 2035 cm^{-1}, and the ^{31}P NMR doublet centred at 40.8 ppm ($^1J_{Rh-P}$ = 166 Hz) indicates equivalent carbonyl and triphenylphosphine ligands. Thus **4** should have the same structure as other heterotrinuclear complexes previously reported, in which the entering fragment (*i.e.* HgI) is bonded to the sulphur atoms already coordinated to the rhodium atoms (Fig. 4) [11c].

When the reaction is carried out in a molar ratio (1 : 1), mixtures of the starting material and **4** are formed. Since a second equivalent of HgI_2 is necessary to complete the reaction, the mercury(II) iodide also acts as iodide abstractor to allow the coordination of the "HgI" fragment.

2.4. Reaction with methyl trifluoromethanesulphonate (triflate)

Complex **1** reacts with methyl triflate to give the cationic trinuclear aggregate $[Rh_3(\mu_3\text{-}C_7H_4NS_2)_2(CO)_3(PPh_3)_3][CF_3SO_3]$ [11c]. The reaction overall indicates a net loss of a bridging ligand, suggesting electrophilic attack of the Me^+ on the coordinated benzo-

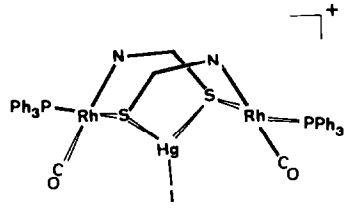

Fig. 4. Proposed structure of the trinuclear aggregate $[(PPh_3)_2(CO)_2Rh_2(\mu_3\text{-}C_7H_4NS_2)_2(HgI)]^+$ (**4**).

thiazol-2-thiolate ligand instead of on the rhodium atoms.

$$3[\{Rh(\mu\text{-}C_7H_4NS_2)(CO)(PPh_3)\}_2] + 2CF_3SO_3Me \longrightarrow 2[Rh_3(\mu_3\text{-}C_7H_4NS_2)_2(CO)_3(PPh_3)_3][CF_3SO_3] + 2CH_3\text{-}C_7H_4NS_2$$

2-(Thiomethyl)benzothiazole was detected by mass spectrum analysis electron impact (EI) of the residue after isolation of the trinuclear complex. Hence, elimination of the ligand as the methyl derivative and the ability of the dinuclear complex to act as the ligand for metal fragments of the type *cis*-RhL_2^+ is the origin of the formation of the trinuclear complex.

In conclusion, the complex $[\{Rh(\mu\text{-}C_7H_4NS_2)(CO)(PPh_3)\}_2]$ (**1**) reacts with electrophiles following two different reactivity patterns. Halogens and methyl iodide react with the basic rhodium atoms by oxidative addition reactions whereas mercury(II) iodide reacts with coordinated exocyclic sulphur atoms of the bridging ligand to form a heterotrinuclear aggregate. Similarly, methyl triflate methylates the benzothiazole-2-thiolate ligands, giving rise to a trinuclear aggregate as a consequence of the removal of a bridge.

3. Experimental details

3.1. General comments

All the reactions were carried out under dry dinitrogen using Schlenk techniques. Isolation of the complexes was performed in air. Solvents were dried by standard methods and distilled under dinitrogen immediately prior to use.

^1H and $^{31}P\{^1H\}$ NMR spectra were recorded on a Varian XL-200 spectrometer operating at 200.057 MHz and 80.984 MHz respectively. Chemical shifts are reported in parts per million relative to tetramethylsilane and phosphoric acid (85%) as external references. IR spectra (range, 4000–200 cm^{-1}) were recorded on a Perkin–Elmer 783 spectrometer using Nujol mulls between polyethylene sheets or in solution in NaCl windows. Elemental analyses were performed with a Perkin–Elmer 240-B microanalyser. Conductivities were measured in approximately 5×10^{-4} mol cm^{-3} acetone solutions using a Phillips 9501/01 conductimeter. Mass spectra were recorded with a VG Autospec double-focusing mass spectrometer using FAB or EI methods. Ions were produce with the standard Cs^+ gun at about 30 kV; 3-nitrobenzyl alcohol (NBA) was used as matrix. $[\{Rh(\mu\text{-}C_7H_4NS_2)(CO)(PPh_3)\}_2]$ (**1**) was prepared by a previously reported method [11a].

3.2. Synthesis of $[\{Rh(\mu\text{-}C_7H_4NS_2)(COCH_3)(I)(PPh_3)\}_2] \cdot CH_2Cl_2$ (2)

A suspension of **1** (0.2 g, 0.178 mmol) in methyl iodide (10 ml) was stirred for 15 min to give a red–brown solution. A red solid began to precipitate as the reaction proceeded. After 3 h the solid was filtered, washed with diethyl ether and dried under vacuum. Recrystallization from dichloromethane–hexane gave the complex as red crystals (0.154 g; 62%). Anal. Found: C, 44.14; H, 3.32; N, 1.67. $C_{55}H_{46}Cl_2I_2N_2O_2P_2Rh_2S_4$ calc.: C, 44.40; H, 3.11; N, 1.88%. IR (CH_2Cl_2): ν(CO) 1720 cm^{-1}. ^1H NMR ($CDCl_3$, 293 K): δ 8.60 (d, $C_7H_4NS_2$), 7.7–7.1 (m, PPh_3 and $C_7H_4NS_2$), 3.10 (s, $COC\underline{H}_3$), 2.92 (s, $CHC\underline{H}_3$). $^{31}P\{^1H\}$ NMR ($CDCl_3$, 293 K): δ 40.3 (d, $^1J_{Rh-P} = 157$ Hz), 35.1 (d, $^1J_{Rh-P} = 140$ Hz). MS (FAB +): m/z (%) 1402 (8, M^+), 1274 (12, $M^+ - I$), 1235 (9, $M^+ - C_7H_4NS_2$), 702 (21, $M/2^+ + H$), 701 (12, $M/2^+$), 574 (97, $M/2^+ - I$), 531 (100, $M/2^+ - I - COCH_3$).

3.3. Synthesis of $[\{Rh(C_7H_4NS_2)I_2(CO)(PPh_3)\}_n]$ (3)

A solution of iodine (3.5 ml, 0.06 mol l^{-1}, 0.21 mmol) in dichloromethane was added to an orange solution of **1** (0.112 g, 0.1 mmol) in dichloromethane (10 ml) to give a red–brown solution in 5 min. Evaporation of the solution under vacuum to about 2 ml gave the complex as a red–brown solid; the precipitation was completed by addition of diethyl ether (10 ml) and then the solid was filtered, washed with diethyl ether and dried under vacuum (0.138 g; 85%). Anal. Found: C, 38.21; H, 2.27; N, 1.65. $C_{26}H_{19}I_2NOPRhS_2$ calc.: C, 38.39; H, 2.35; N, 1.72%. IR (CH_2Cl_2): ν(CO) 2080 cm^{-1}. $^{31}P\{^1H\}$ NMR ($CDCl_3$, 293 K): δ 39.0 (d, $^1J_{Rh-P} = 93$ Hz).

3.4. Synthesis of $[(PPh_3)_2(CO)_2Rh_2(\mu_3\text{-}C_7H_4NS_2)_2(HgI)][HgI_3]$ (3)

Solid mercury(II) iodide (0.091 g, 0.2 mmol) was added to a solution of **1** (0.112 g, 0.1 mmol) in dichloromethane (10 ml). The mixture was stirred for 1 h to give an orange–brown solution. Evaporation under vacuum to 2 ml and slow addition of diethyl ether gave the complex as a yellow microcrystalline solid which was filtered off, washed with diethyl ether and vacuum dried (0.147 g; 78%). Anal Found: C, 30.99; H, 1.99; N, 1.20. $C_{52}H_{38}Hg_2I_4N_2O_2P_2Rh_2S_4$ calc.: C, 30.80; H, 1.88; N, 1.38%. Λ_M: 122 Ω^{-1} cm^2 mol^{-1}. IR (CH_2Cl_2): ν(CO) 2035 cm^{-1}. ^1H NMR ($CDCl_3$, 293 K): δ 8.11 (d, $C_7H_4NS_2$), 7.6–7.1 (m, PPh_3 and $C_7H_4NS_2$), 7.0–6.8 (m, $C_7H_4NS_2$). $^{31}P\{^1H\}$ NMR ($CDCl_3$, 293 K): δ 40.8 (d, $^1J_{Rh-P} = 166$ Hz). MS (FAB +): m/z (%) 1446 (9, M^+), 1062 (10, $M^+ - HgI - 2CO$), 952 (16, $M^+ - HgI - C_7H_4NS_2$), 896 (10, $M^+ -$

$HgI - 2CO - C_7H_4NS_2$), 531 (100, "$Rh(C_7H_4NS_2)(PPh_3)$"). MS (FAB −): *m/z* (%) 583 (100, HgI_3^-).

3.5. Reaction of 1 with methyl trifluoromethanesulphonate

To a solution of **1** (0.112 g, 0.1 mmol) in dichloromethane (10 ml) methyl triflate (7.31 μl, 0.06 mmol) was added. The solution turned deep red in 30 min. Concentration of the solution to about 2 ml and addition of diethyl ether (30 ml) gave a garnet solid (70%) identified as $[Rh_3(\mu_3\text{-}C_7H_4NS_2)_2(CO)_3(PPh_3)_3][CF_3SO_3]$ by its spectroscopic properties [11b]. The mother liquor was concentrated, passed through a short column of silica gel and evaporated to dryness. The mass spectrum (EI) of the residue shows 2-(methylthio)benzothiazol as the main component. MS (EI, 70 eV): *m/z* (%) 181 (100, L^+), 166 (10, $L^+ - Me$), 148 (60, $L^+ - SMe$), 108 (34, $L^+ - SMe - CN$).

3.6. X-ray crystallographic study of $[\{Rh(\mu\text{-}C_7H_4NS_2)(COCH_3)(I)(PPh_3)\}_2] \cdot CH_2Cl_2$ (2)

3.6.1. Crystal data

$C_{55}H_{46}Cl_2I_2N_2O_2P_2Rh_2S_4$; $M = 1487.69$; monoclinic; space group, $C2/c$; $a = 21.443(1)$, $b = 16.303(1)$, $c = 17.7329(6)$ Å, $\beta = 111.023(3)°$; $V = 5786.5(5)$ Å^3; $Z = 4$; $D_c = 1.708$ Mg m^{-3}; F (000) = 2920; λ(Mo Kα) = 0.710 69 Å; $\mu = 19.44$ cm^{-1}; $T = 295$ K.

3.6.2. Data collection and processing

A Siemens AED-2 diffractometer with monochromated Mo Kα radiation was used. A red irregular block 0.228 × 0.331 × 0.580 mm was mounted on a glass fibre. 8910 Intensities were registered to $2\theta_{max}$ 47° (ω–2θ scan technique). Averaging equivalents gave 4241 unique reflections, of which 3889 with $F \geqslant 4.0\sigma(F)$ were used for all calculations (program system SHELX76) [39]. Cell constants were refined from setting angles of 52 reflections in the 2θ range 20–35°. Three standard reflections were monitored every hour as a check on crystal and instrument stability. Data were corrected for Lorentz and polarization effects. An semi-empirical absorption correction was also applied [40] (transmission factor, 0.813, 0.937).

3.6.3. Structure solution and refinement

The structure was solved by Patterson methods and extended by difference syntheses. Atoms were refined isotropically first, and in subsequent cycles with anisotropic thermal parameters for all the non-hydrogen atoms (excepting those involved in solvent disorder). Hydrogen atoms were found in difference maps and included in the last cycles of refinement using a riding model with a common thermal parameter. At this stage, several residual peaks assignable to a highly disordered solvent molecule were observed. The three most intense showed reasonable geometry for a CH_2Cl_2 molecule, but some peaks still remained in the Fourier map. Some attempts were made to model these electronic density residuals, bearing in mind the solvents used during the crystallization process. However no model was clear and eventually all the remaining peaks with more than 2 electrons Å^{-3} (three peaks) and a

TABLE 2. Atomic coordinates and equivalent isotropic displacement coefficients for the non-hydrogen atoms of the complex $[\{Rh(\mu\text{-}C_7H_4NS_2)(COCH_3)(I)(PPh_3)\}_2]$ (2) CH_2Cl_2

Atom	$x \times 10^5$	$y \times 10^5$	$z \times 10^5$	U_{eq} [a] $\times 10^4$ (Å^2)
Rh	4730(1)	22965(2)	18286(1)	342(1)
I	1056(1)	18999(2)	2735(1)	561(1)
S(1)	6810(4)	22011(5)	32398(5)	374(3)
S(2)	9842(5)	4603(6)	39567(6)	543(4)
P	15637(4)	25556(6)	19114(5)	360(3)
N	7260(14)	8467(18)	24597(16)	409(11)
C(1)	3174(17)	35072(23)	17621(21)	435(14)
C(2)	−2436(21)	38490(26)	10315(24)	635(18)
O	6435(13)	39380(16)	23008(17)	552(11)
C(3)	7955(16)	11473(21)	31618(19)	395(12)
C(4)	8143(18)	66(23)	25079(21)	469(14)
C(5)	7573(20)	−5265(27)	18571(26)	603(17)
C(6)	8607(23)	−13461(31)	20179(32)	766(22)
C(7)	10104(24)	−16580(30)	27833(36)	828(24)
C(8)	10684(23)	−11580(27)	34346(30)	707(20)
C(9)	9705(19)	−3280(24)	32821(23)	514(15)
C(10)	19231(17)	18184(21)	14070(20)	400(13)
C(11)	17548(21)	10055(24)	14038(24)	549(17)
C(12)	20366(25)	4115(27)	10589(28)	704(21)
C(13)	24638(31)	6548(33)	6949(34)	937(30)
C(14)	26409(33)	14773(36)	6925(37)	1047(34)
C(15)	23668(24)	20606(28)	10454(29)	687(21)
C(20)	21783(17)	26033(21)	29391(20)	400(13)
C(21)	27518(18)	21308(24)	31778(23)	501(15)
C(22)	32268(20)	22239(27)	39503(25)	636(17)
C(23)	31233(22)	27704(29)	44834(25)	648(18)
C(24)	25518(21)	32377(26)	42486(23)	563(16)
C(25)	20786(19)	31550(23)	34855(22)	464(14)
C(30)	16783(17)	35413(22)	14779(20)	420(13)
C(31)	21792(21)	40889(25)	18946(25)	573(17)
C(32)	22558(26)	48272(27)	15538(29)	721(21)
C(33)	18307(27)	50238(27)	7873(28)	699(22)
C(34)	13384(24)	44850(29)	3613(27)	674(20)
C(35)	12615(20)	37343(25)	7004(23)	545(16)
Cl(1)[b]	50794(25)	13992(29)	33222(27)	1600(18)
Cl(2)[b]	52917(41)	13780(50)	14250(48)	1336(26)
Cl(3)[b]	38166(46)	8697(58)	21861(53)	1628(32)
C(40)[b]	50000	7962(121)	25000	1244(58)
C(41)[b]	44385(163)	9694(194)	20876(186)	1482(103)
C(42)[b]	43844(132)	8465(172)	30373(156)	1200(79)

[a] Equivalent isotropic U defined as one third of the trace of the orthogonalized U_{ij} tensor.

[b] Atoms included to take account of disordered solvent, refined with isotropic thermal parameters.

TABLE 3. Full experimental details for the X-ray analysis of the compound $[\{Rh(\mu\text{-}C_7H_4NS_2)(COCH_3)I(PPh_3)\}_2]\cdot CH_2Cl_2$

Crystal data	
Formula	$C_{54}H_{44}I_2N_2O_2P_2Rh_2S_4\cdot CH_2Cl_2$
Molecular weight	1487.69
Crystal habit	Irregular transparent red block
Size (mm)	$0.228\times0.331\times0.580$
Symmetry	Monoclinic; $C2/c$
Unit-cell determination	Least-squares fit to 52 reflections. ($20\leqslant 2\theta\leqslant 35°$)
Unit-cell dimensions	
a, b, c (Å)	21.443(1), 16.303(1), 17.7329(6)
β (°)	111.023(3)
Packing: V (Å^3), Z	5786.5(5), 4
D (g cm^{-3}), F (000)	1.708, 2920
Experimental data	
Radiation and technique	4-Circle Siemens AED diffractometer
	Graphite monochromated Mo-Kα (λ = 0.710 69 Å) Bisecting geometry
Temperature (K)	295
Collection mode (range)	ω–2θ scan ($3\leqslant 2\theta\leqslant 47°$)
Number of reflections	
Measured	8910 (h, −12 12; k, −14 14; l, 0 16)
Unique	4241 (merging R factor, 0.0162)
Observed	3889 ($F\geqslant 4.0\sigma(F)$)
Standard reflections	Three standards measured every 55 min approximately. No variation observed
Absorption correction	Ψ scan method [40]
Minimum transmission factor; maximum transmission factor	0.813, 0.937
μ (cm^{-1}), μR	19.44, 0.350
Solution and refinement	
Computer	SHELX76 system, μVAX 3400
Solution mode	Patterson
Refinement	Full-matrix least-squares method on F values. Observed reflections only
Hydrogen atoms	From observed positions. Riding model with a common thermal parameter
Number of parameters	331
Weighting scheme	$w = 1.000/\sigma^2(F) + 0.000126F^2$
ΔF final (electrons Å^{-3})	0.76 (close to the disordered solvent)
Maximum thermal value (Å^2)	U_{33} (O(11)) = 0.126 4(26)
R, wR (observed data)	0.02358, 0.0350
R indices (all data)	0.0295, 0.0356
Goodness of fit	1.85
Largest Δ/σ, mean Δ/σ	0.001, 0.000
Data-to-parameter ratio	11.7 to 1

Atomic scattering factors are taken from the *International Tables for X-ray Crystallography* [41]; neutral atoms. Anomalous dispersion applied for Rh, S and P atoms.

plausible dichloromethane geometry were include in the final calculation. The final R value was 0.0258, with $R_w = 0.0292$. The weighting scheme was $w = k/\sigma^2(F) + gF^2$, with $k = 1.00$ and $g = 0.000\,126$; 331 refined parameters; maximum $\Delta/\sigma < 0.001$; maximum $\Delta\rho$, 0.76 electrons Å^{-3}, situated close to the disordered solvent. Atomic scattering factors, corrected for anomalous dispersion, were taken from ref. 41. Final atomic coordinates are given in Table 2 and details of the structure determination in Table 3.

Additional material available from the Cambridge Crystallographic Data Centre comprises H atom coordinates, thermal parameters and remaining bond lengths and angles.

Acknowledgments

We wish to thank Comisión Interministerial de Ciencia y Tecnologia and Generalitat de Catalunya for financial support (project QFN92-4311) and Diputación General de Aragón for a fellowship to J.J.P.T.

References

1 See for example Z. He, S. Nefedov, N. Lugan, D. Neibecker and R. Mathieu, *Organometallics, 12* (1993) 3837; J.B. Tommasino, D. Montauzon, X.D. He, A. Maisonnat, R. Poilblanc, J.N. Verpeaux and C. Amatore, *Organometallics, 11* (1992) 4150, M.H. Chisholm, K. Folting, J.C. Huffman, K.S. Kramer and R.J. Tatz,

Organometallics, 11 (1992) 4029; S. Lo Schiavo, E. Rotondo, G. Bruno and F. Faraone, *Organometallics, 10* (1991) 1613.
2 (a) R. Usón, A. Laguna, M. Laguna, J. Jiménez and P.G. Jones, *J. Chem. Soc., Dalton Trans.*, (1991) 1361; (b) A. Laguna, M. Laguna, J. Jiménez, F.J. Lahoz and E. Olmos, *J. Organomet. Chem., 435* (1992) 235; (c) H. Schmidbaur, Th. Pollok, F.E. Wagner, R. Bau, J. Riede and G. Müller, *Organometallics, 5* (1986) 566.
3 R.J. Puddephatt, *J. Chem. Soc. Rev.*, (1983) 99; B. Chaudret, B. Delavaux and R. Poilblanc, *Coord. Chem. Rev., 86* (1988) 191.
4 (a) A. Mayanza, J.J. Bonnet, J. Galy, P. Kalck and R. Poilblanc, *J. Chem. Res. (s),* (1980) 146; *J. Chem. Res. (M)* (1980) 2101; (b) C. Claver, J. Fis, P. Kalck and J. Javel, *Inorg. Chem., 26* (1987) 3479; (c) T.A. Wark and D.W. Stephan, *Inorg. Chem., 26* (1987) 363; (d) F.A. Cotton, P. Lahuerta, J. Latorre, M. Sanau, I. Solana and W. Schowotzer, *Inorg. Chem. 27* (1988) 2131; (e) D. Rosenhein and S.W. McDonald, *J. Organomet. Chem., 345* (1988) 143.
5 (a) M.T. Pinillos, A. Elduque, J.A. López, F.J. Lahoz and B.E. Man, *J. Chem. Soc., Dalton Trans.*, (1991) 2807; (b) M.T. Pinillos, A. Elduque, J.A. López, F.J. Lahoz and L.A. Oro, *J. Chem. Soc., Dalton trans.*, (1991) 1391.
6 (a) T.G. Schenck, J.M. Downes, C.R.C. Milnen, P.B. Mackenzie, H. Boucher, J. Whelan and B. Bosnich, *Inorg. Chem., 24* (1985) 2334; (b) T.G. Schenck, C.R.C. Milnen, J.F. Sawyer and B. Bosnich, *Inorg. Chem., 24* (1985) 2338.
7 (a) G. Bruno, S. Lo Schiavo, E. Rotondo, C.G. Arena and F. Faraone, *Organometallics, 8* (1989) 886; (b) E. Rotondo, S. Lo Schiavo, G. Bruno, C.G. Arena, R. Gobetto and F. Faraone, *Inorg. Chem., 28* (1989) 2944; (c) C.G. Arena, F. Faraone, M. Lanfredi, E. Rotondo and A. Tiripicchio, *Inorg. Chen., 31* (1992) 4797.
8 (a) X.D. He, A. Maisonnat, F. Dahan and R. Poilblanc, *Organometallics, 8* (1989) 2618; (b) M.D. Rausch, W.C. Spink, J.L. Atwood, A.J. Baskar and S.G. Botl, *Organometallics, 8* (1989) 2677; (c) X.D. He, A. Maisonnat, F. Dahan and R. Poilblanc, *New J. Chem., 14* (1990) 313; (d) X.D. He, A. Maisonnat, F. Dahan and R. Poilblanc, *Organometallics, 10* (1991) 2443.
9 (a) S.A.R. Knox, *J. Organomet. Chem. 400* (1990) 255; (b) R.N. Vrtis, S.G. Bott and S.J. Lippard, *Organometallics, 11* (1992) 270; (c) M.A. Ciriano, M.A. Tena and L.A. Oro, *J. Chem. Soc., Dalton Trans.*, (1992) 2123.
10 M.A. Ciriano, J.J. Pérez-Torrente and L.A. Oro, *J. Organomet. Chem., 445* (1993) 273.
11 (a) M.A. Ciriano, F. Viguri, J.J. Pérez-Torrente, F.J. Lahoz, L.A. Oro, A. Tiripicchio and M. Tiripicchio-Camellini, *J. Chem. Soc., Dalton Trans.*, (1989) 25; (b) M.A. Ciriano, J.J. Pérez-Torrente, F. Viguri, F.J. Lahoz, L.A. Oro, A. Tiripicchio and M. Tiripicchio-Camellini, *J. Chem. Soc., Dalton Trans.*, (1990) 1493; (c) M.A. Ciriano, J.J. Pérez-Torrente, L.A. Oro, A. Tiripicchio and M. Tiripicchio-Camellini, *J. Chem. Soc., Dalton Trans.*, (1991) 255.
12 M.A. Ciriano, S. Sebastian, L.A. Oro, A. Tiripicchio, M. Tiripicchio-Camellini and F.J. Lahoz, *Angew. Chem., Int. Edn. Engl., 27* (1988) 402.
13 M.A. Ciriano, J.J. Pérez-Torrente, F.J. Lahoz and L.A. Oro, *J. Organomet. Chem., 455* (1993) 225.
14 M.A. Ciriano, J.J. Pérez-Torrente, F.J. Lahoz and L.A. Oro, *Inorg. Chem., 31* (1991) 969.
15 A. Bondi, *J. Phys. Chem.*, 68 (1964) 441.
16 (a) M.A. Bennett, J.C. Jeffery and J.C. Robertson, *Inorg. Chem., 20* (1981) 330; (b) G.K. Anderson and R.J. Cross, *Acc. Chem. Res., 17* (1984) 74.
17 B.M. Louie, S.J. Rettig, A. Storr and J. Trotter, *Can. J. Chem., 63* (1985) 3019.
18 H. Adams, N.A. Bailey, B.E. Mann, C.P. Manuel and A.G. Kent, *J. Chem. Soc., Dalton Trans.*, (1988) 489.
19 C. Bianchini, A. Meli, M. Peruzzini and F. Vizza, *Organometallics, 10* (1991) 820.
20 S. Jeannin, Y. Jeannin and G. Lavigne, *J. Cryst. Mol. Struct., 7* (1977) 241; S. Jeannin, Y. Jeannin and G. Lavigne, *Trans. Met. Chem., 1* (1976) 195.
21 M.B. Hursthouse, O.F.Z. Khan, M. Mazid, M. Motevalli and P. O'Brien, *Polyhedron, 9* (1990) 541.
22 J.H. Yamamoto, W. Yoshida and C.M. Jensen, *Inorg. Chem., 30* (1991) 1353.
23 J.P. Chesick and J. Donohue, *Acta Crystallogr. Sect. B, 27* (1971) 1441.
24 F.H. Allen, J.E. Davies, J.J. Galloy, O. Johnson, O. Kennard, C.F. Macrae, E.M. Mitchell, G.F. Mitchell, J.M. Smith and D.G. Watson, *J. Chem. Inf. Comput. Sci., 31* (1991) 187.
25 A.G. Orpen, L. Brammer, F.H. Allen, O. Kennard, D.G. Watson and R. Taylor, *J. Chem. Soc., Dalton Trans.*, (1989) S1.
26 D.L. Egglestone, M.C. Baird, C.J.C. Lock and G. Turner, *J. Chem. Soc., Dalton Trans.*, (1977) 1576.
27 J.A. Cabeza, V. Riera, M.A. Villa-García, L. Ouahab and S. Triki, *J. Organomet. Chem., 441* (1992) 323.
28 K.S.Y. Lau, Y. Becker, F. Huang, N. Baenziger and J.K. Stille, *J. Am. Chem. Soc., 99* (1977) 5664.
29 C. Bianchini, A. Meli, M. Peruzzini, A. Vacca and F. Zanobini, *Organometallics, 6* (1987) 2453.
30 J.V. Heras, E. Pinilla and P. Ovejero, *J. Organomet. Chem., 332* (1987) 213.
31 G.J.J. Steyn, A. Roodt and J.G. Leipoldt, *Inorg. Chem., 31* (1992) 3477; J.A. Venter, J.G. Leipoldt and R. van Eldik, *Inorg. Chem., 30* (1991) 2207.
32 J.P. Collman, L.S. Hegedus, J.R. Norton and R.G. Finke, *Principles and Applications of Organotransition Metal Chemistry,* University Science Books, Mill Valley, CA, 1987.
33 F.J. Garcia-Alonso, A. LLamazares, V. Riera and M. Vivanco, *Organometallics, 11* (1992) 2826.
34 J.P. Collman, R.K. Rothrock, R.G. Finke, E.J. Moore and F. Rose-Munch, *Inorg. Chem., 21* (1982) 146.
35 (a) J.H. Yamamoto, W. Yoshida and C.M. Jensen, *Inorg. Chem., 30* (1991) 1353; (b) G.P.A. Yap and C.M. Jensen, *Inorg. Chem., 32* (1992) 4823.
36 D.F. Steele and T.A. Stephenson, *J. Chem. Soc., Dalton Trans.*, (1972) 2161.
37 A. Tiripicchio, F.J. Lahoz, L.A. Oro and M.T. Pinillos, *J. Chem. Soc., Chem. Commun.*, (1984) 936; M.T. Pinillos, A. Elduque and L.A. Oro, *Polyhedron, 11* (1992) 1007.
38 J.L. Dawes and R.D.W. Kemmitt, *J. Chem. Soc. A,* (1968) 2093.
39 G.M. Sheldrick, SHELX Program for Crystal Structure Determination, University of Cambridge, Cambridge, 1976.
40 A.C.T. North, D.C. Philips and F.S. Mathews, *Acta Crystallogr., Sect. A, 24* (1968) 351.
41 *International Tables for X-ray Crystallography,* Vol. 4, Kynoch, Birmingham, 1974.